PERGAMON

Journal of Asian Earth Sciences 20 (2002) 247–253

Journal of Asian Earth Sciences

www.elsevier.com/locate/jseaes

15th INTERNATIONAL HIMALAYA–KARAKORAM–TIBET WORKSHOP

# Tarim underthrust beneath western Kunlun: evidence from wide-angle seismic sounding

Li Qiusheng[a,b,*], Gao Rui[a], Lu Deyuan[a], Li Jingwei[b], Fan Jingyi[b], Zhang Zhiying[b], Liu Wen[b], Li Yingkang[b], Yan Quanren[b], Li Dexing[a], Wide Angle team

[a]*Lithosphere Research Center of Chinese Academy of Geological Science, Beijing 100037, People's Republic of China*
[b]*562 Comprehensive Institute of Chinese Academy of Geological Science, Sanhe, Hebei 065201, People's Republic of China*

Received 29 August 2000; accepted 24 April 2001

**Abstract**

This paper describes the results of a wide-angle seismic profile, over 700 km long, across the southern margin of the Tarim Basin. A crustal structure that best fits the observed data, that tests and verifies the earlier discovery that the crystalline basement dips southward from the area of the petroleum industry seismic reflection profiling and geological investigation is presented. The profile also reveals that the Moho dips southward beneath the southern Tarim, at an angle in concordance to that of the crystalline basement. This result is thought to be the first evidence for the underthrusting of the Tarim crust beneath the western Kunlun. Additional evidence of underthrusting is that the relatively weak western Kunlun crust has contracted, and expressed by a lower crust, which is more than 20 km thick, with an uplift of the Kunlun basement, accompanied by northward-directed thrusts. 

*Keywords*: Tibet; Asian tectonics; seismicprofiles; data aquisition

## 1. Introduction

A great deal of attention has been paid to the Indo-Asian collision in southern Tibet during the past three decades (e.g. Dewey and Burke, 1973; Molnar, 1984; Tapponnier et al., 1986; Zhao et al., 1993; Molnar et al., 1993; Nelson et al., 1996; Yuan et al., 1997). The contribution of the Tarim Block to the Himalayan–Tibetan orogenic system was not appreciated until Layon-Caen and Molnar (1984) suggested the Tarim Block has been underthrust southward beneath the western Kunlun during the Cenozoic, for a distance of at least 80 km. In recent years, this conclusion has been further supported by later geological investigations (Cowgill et al., 1998) and subsurface data from the southwest Tarim Basin (Jia, 1997), but the deep structure still remained unclear in the area of southern Tarim and western Kunlun until the present study.

A crustal reconnaissance by seismic refraction/wide-angle reflection profile, with a length of 700 km, designed to investigate the structure of the crust and to provide a detailed velocity-depth function for Xinjiang Global Geosciences Transect (GGT), was conducted by the Chinese Academy of Geological Science (CAGS) during August–October 1997. The focus of this paper is the determination of the crustal structure of the transition zone between the Tarim Basin and the western Kunlun Mountains.

## 2. Tectonic setting and previous geophysical studies

The refraction/wide-angle profile, approximately perpendicular to the regional tectonic strike, was designed to pass through three main geotectonic domains, defined as the western Kunlun Terrane, the Tiekelik Terrane and the Tarim Basin (Liu and Fu, 1999). The western Kunlun Terrane, where the basement consists of Middle Proterozoic gneiss and schist, lies between the Kuda Fault and Kangxiwa Fault. The Tiekelik Terrane is bounded by the Kuda Fault in the south and by the Frontal Thrust Fault in the north. The oldest unit outcropping in the Tiekelik Terrane is the Lower Proterozoic schist and gneiss, with high metamorphic grade and strong migmatization (Matte et al., 1996). Most of the Tarim Basin is covered by sediments of the Quaternary system, except for the area of the Bachu uplift, where outcrops of Paleozoic rock are exposed. Based on the surface geological and subsurface geophysical, as well as drill-hole data, the Tarim Basin was a large marine

* Corresponding author. Address: Lithosphere Research Center of Chinese Academy of Geological Science, Beijing 100037, People's Republic of China.
*E-mail address:* liqiusheng@cags.cn.net (Li Qiusheng).

1367-9120/02/$ - see front matter 
PII: S1367-9120(01)00057-8

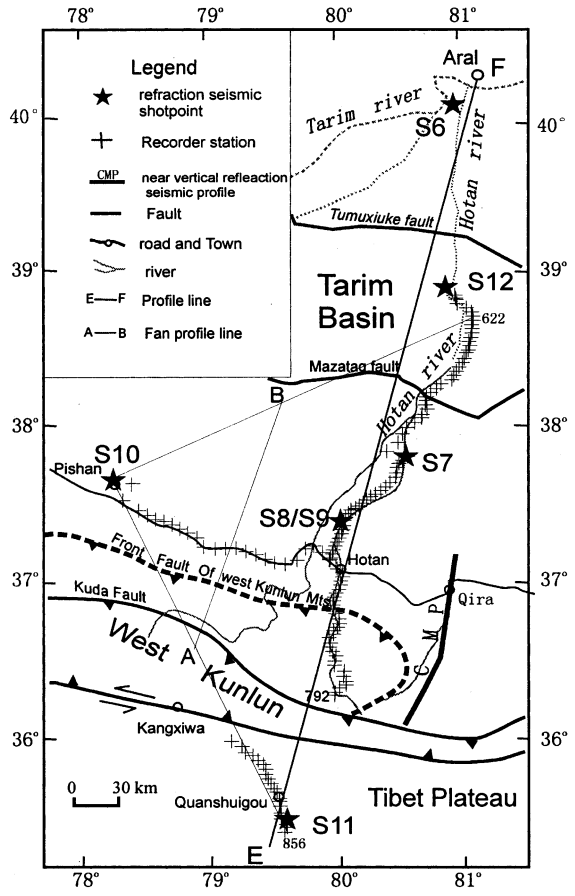


Fig. 1. Layout of explosive seismic sounding experiment and tectonic framework.

cratonic basin during the Paleozoic, and an inland basin during the Mesozoic, and has remained tectonically stable between the uplift of the Tibetan Plateau and the Tianshan. Recent literature usually divides the Tarim Basin, from south to north, into the Southwest Depression, the Central Uplift and the Northern Depression. Numerous publications have described the Southwest and the Northern depressions as foreland basins (Ding and Tang, 1996; Jia, 1997).

Previous seismological studies (surface wave and tomography) estimate the average thickness of the crust beneath the Tarim Basin as 40–50 km, and the crust of the western Kunlun orogenic region as more than 50 km. The petroleum industry seismic profile from the southern Tarim to western Kunlun revealed that the basement of southwest Tarim dips gently southward beneath the western Kunlun. From north to south, the gravity map shows a gradual decrease in the gravity values from −150 to −450 mGal. The dip of the basement in the southern Tarim and the uplift of the basement, with northward-directed thrusting in the northern slopes of the Kunlun, covered by the Neogene of the Tarim Basin, were thought to provide primary geophysical evidence that the Tarim Basin had been thrust beneath the western Kunlun.

## 3. Data collection and preprocessing

The geographic coverage of this paper is 35.4°–40.4°N, 79.5°–80.5°E (Fig.1). Apart from some work in the western Kunlun Mountains, most of this seismic profiling project was conducted in the Taklimakan Desert, which made fieldwork very difficult. The seismic reflection profile commenced in the north at Aral (40°33′16.4″N, 81°14′49.4″E) near the Tarim River, crossed the Taklimakan Desert along the Hotan River and the western Kunlun Mountains to the Tibetan Plateau, ending at Quanshuigou (35°31′37.4″N, 79°32′01.3″E). The main seismic profile, extending across the Tarim Basin and the Western Kunlun Mountains has a total length of 700 km (Fig.1, EF).

Seven shots (Table 1) were each recorded by a total of 120 portable cassette recorders (32 digital and 88 analog), each with a three-component sensor. Seismic energy was generated by multiple borehole explosions, with the exception of the shot at Sanzhan (Tabel 1, S12), which due to problems of accessibility for the drilling equipment, was detonated in two artificially dug pits. Shotpoints were spread from 50 to 150 km apart. A total of 10,500 kg of explosive charge was distributed among seven shots, and each shot varied from 1000 to 2500 kg, depending on the site conditions and the maximum distance from the shot recorders. The recorders were spaced at an average distance of 3 km to receive the seismic energy on a longitudinal or a fan/broadside layout, in which the acquisition of the near or over-critical reflection is mainly optimized. For alternate shots the recorders were arranged as a reversed or overlapping system. The recorder array was spread along the profile for a distance of more than 300 km.

The shots on Table 1 were observed with a longitudinal

Table 1
Shot-point data (the results from shot numbers S1 to S5, located in the Tianshan area, have been published elsewhere)

| Shot name | Shot no | Latitude | Longitude | Altitude (m) | Shot time (UTC): 1997 | Size (kg) |
|---|---|---|---|---|---|---|
| Aral | S6 | 40 24.248 | 80 51.200 | 1025 | Sep.12, 14:00:06.606 | 1500 |
| Sanzhan | S12 | 38 50.800 | 80 48.453 | 1140 | Sep.15, 13:00:06.950 | 1000 |
| Erízhan | S7 | 37 50.532 | 80 26.702 | 1250 | Sep.12, 13:00:06.413 | 1500 |
| Hotan-1 | S8 | 37 25.400 | 79 58.075 | 1290 | Sep.02, 13:00:06.245 | 1000 |
| Hotan-2 | S9 | 37 25.400 | 79 58.075 | 1290 | Sep.07, 13:00:06.348 | 1500 |
| Pishan | S10 | 37 41.403 | 78 14.051 | 1300 | Sep.07, 14:00:05.083 | 1500 |
| Quanshuigou | S11 | 35 31.623 | 79 32.021 | 4800 | Sep.02, 14:00:07.094 | 2500 |

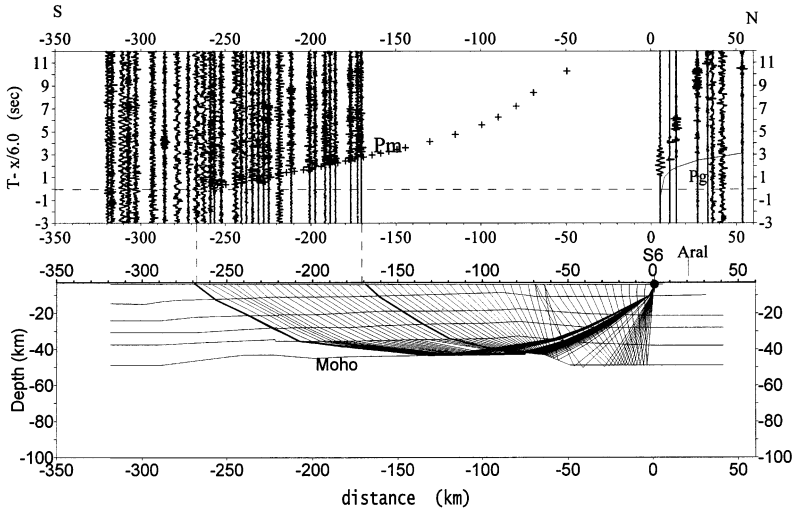


Fig. 2. Aral Shot: record section and crustal model with ray-tracing. (a) The record section shows a Pm phase from 170 to 260 km. At 170 km the record is blank near the shot point, because of the obstruction of the desert. (b) A crustal model constrained by the measured seismic data. The reflection segment of Pm is under Central Tarim.

layout, except for Pishan (S10) which was designed to be a fan/broadside shotpoint, situated 160 km to the west of Hotan. The recorders were deployed for fan/broadside observation, beginning from Mazatag (No.622) to Quanshuigou (No.856), and extending 380 km from north to south (Fig. 1). The distance of the shot-recorder varied from 150 to 270 km. The midpoints of the paths that seismic wave travelled from fan shot-point to recorder station was projected onto the surface as AB (Fig. 1).

The positions of the shotpoints and recorder stations were measured with an accuracy of 50–100 m, using portable GPS, and were located on a 1:100 000 relief map. All shooting times and seismic wave travel times have been corrected to the UTC (Coordinated Universal Time) base.

The primary data was collected over a recording window length of 5 min for each shot, and selectively sampled from 0–40 s (reduce time, reduce velocity: 6.0 km $s^{-1}$) at 10 ms intervals for P-wave analysis. The data was processed, following the usual scheme in refraction seismic surveys. First the three-component data was decomposed into three single-components, then the vertical component was picked out, and after appropriate filtering (usually 1–8 Hz band pass), was plotted in reduced sections (reduced velocity: 6.0 km $s^{-1}$) with normalized amplitudes, and at several scales, to ensure reliability in phase identification and travel time picking. An irregularity in the fan-record section is that its horizontal axes were drawn from the recorder stations to a relative-point (generally not the shotpoint), usually chosen as the southernmost or northernmost point on the observing array.

## 4. Data description and interpretation procedure

Several refracted/reflected seismic phases were identified in practically all the recorded sections. The phases, named Pg, P4 and Pm, correspond to the energy refracted through the upper crust, and reflections from the middle-lower crust and crust–mantle boundaries, respectively. Additional wide-angle reflections identified in some sections, such as P1, P2 and P3, denote reflections from upper-middle crust.

### *4.1. Aral shot (S6) (Fig. 2)*

Pm appears in the offset range 170–280 km as the first arrival, with ascendant amplitude. The travel time of Pm was matched by a crustal model with a mean velocity of 6.36 km $s^{-1}$, a thickness of 40 ± 2 km and a moderately high velocity (7.0–7.3 km $s^{-1}$) for the lower crust beneath Central Tarim. The upper mantle refraction phase Pn should appear beyond offset at 200 km, but looks particularly weak. It is estimated to have a phase velocity of 7.9 ± 0.2 km $s^{-1}$ if the phase is identified correctly.

### *4.2. Hotan shot (S8, S9) (Fig. 3)*

The primary seismic phases Pg, P4 and Pm (PmP) are marked on the record section. The phase Pg, identified also in other shot record sections, is the first arrival phase in the section, and has a velocity of approximately 6.0 km $s^{-1}$. It suddenly becomes weak at −30 km and arrives early (about 0.5 s), beyond that offset, until −90 km. This abnormality is associated with the northward thrust of Tiekelik Terrane. Within 40 km of the shotpoint, the Pg travel time indicates a zone from the surface to 12–18 km depth with a very low gradient, representing the sedimentary cover.

The P4, a later arrival, appears in the section at 6.5 s, with a 70 km offset, and traceable for a great distance, is interpreted to be a phase from the middle crust/lower crust boundary, at around 35 km depth, in the area of the southern Tarim and west Kunlun.

The Pm phase is easily identified because of its typical

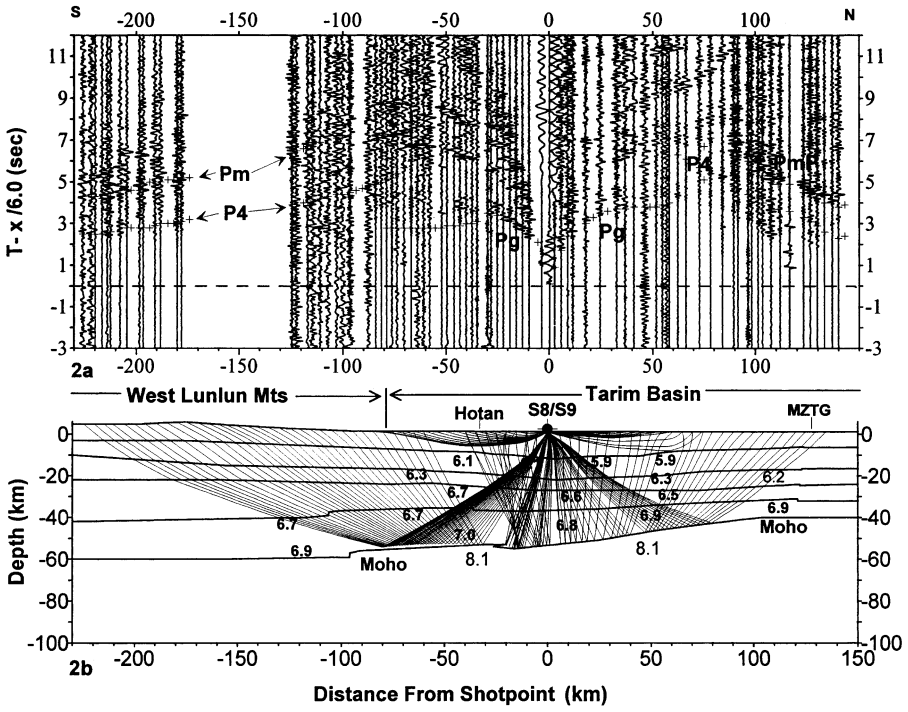


Fig. 3. Hotan shot: record section and crustal model with ray tracing (a) P-wave record section from shots 8 and 9; Pg, basement refraction; Pm, Moho reflection; P4, from the top of lower crust. (b) The raying-tracing diagram. Hotan and Mazatag Hill (MZTG) are marked on the section. The distance axis refers to the distance from the shotpoint to the recorder stations. The upper mantle velocity is assumed to be 8.1 km $s^{-1}$ for forward calculation.

critical reflection characteristics. Comparing its appearance on both sides of a shotpoint, it is found that it has a higher apparent velocity and a sharper wave formation on Tarim Basin side, as opposed to the Pm phase which continues with lower apparent velocity and blunt wavelet, as the seismic waves travel through the western Kunlun. The travel time was successfully modeled, with the Moho dipping southward at a depth varying from 40 to 58 km.

### 4.3. Pishan shot (S10) (Fig. 4)

The Pishan shot was a fan/broadside survey record section (top diagram), designed to constrain the lateral variation of the Moho at the transition zone between the basin and the mountains. Pm, with the traditional feature of the near and post critical reflection, is reliably identified by its first arrival and high-amplitude in the section. The travel time of Pm, observed from fan-sections, is usually used to provide loose constraints on estimates of crustal thickness and mean velocity. In the skeleton model shown in Fig. 4 (lower diagram), it is presumed that the depth of the crust/mantle boundary gradually increases from ~40 km below the southern Tarim Basin to ~60 km below the western Kunlun. This interpretation fits the observed Pm data. In contrast, the Moho becomes flat and shows a slightly northerly dip under the northern slopes of the western Kunlun. This reversal of dip direction is taken to mark the division between the western Kunlun and the Tarim Basin in the later discussion.

### 4.4. Interpretation procedure

The interpretation of data to determine the P wave velocity-depth distribution was accomplished by an iterative combination of forward modeling and travel time inversion. The initial crustal structure model is based on the resolution (depth and layer velocity) of inversion. Geological and geophysical constraints, where available, have also been included in the model. The final model was determined by 2-D forward ray-tracing and synthetic seismogram calculation.

Some traditional inverse methods were used to model the upper crustal structure, based on the Pg arrival, e.g. the Wiechert–Herglotz method. The crustal structure below ~10 km was determined from wide-angle reflections. Modeling of the crust and uppermost mantle was carried out using 2-D forward ray-tracing. The travel time and amplitudes of all the seismic phases were calculated using the SEIS-81 and SEIS-83 programs (Cerveny et al., 1977; Cerveny and Psencik, 1984). Synthetic seismograms have been also calculated using the asymptotic ray theory (Cerveny and Psencik, 1984).

In the technological procedure, the single shot data was modeled first. The segments were then combined into a long model on the designed layout. The model is further constrained by multi-shot data and the general characteristic of the wave field. The accepted resolution for the final model was obtained from the calculated travel time and from the best-fit synthetic seismogram for the observed

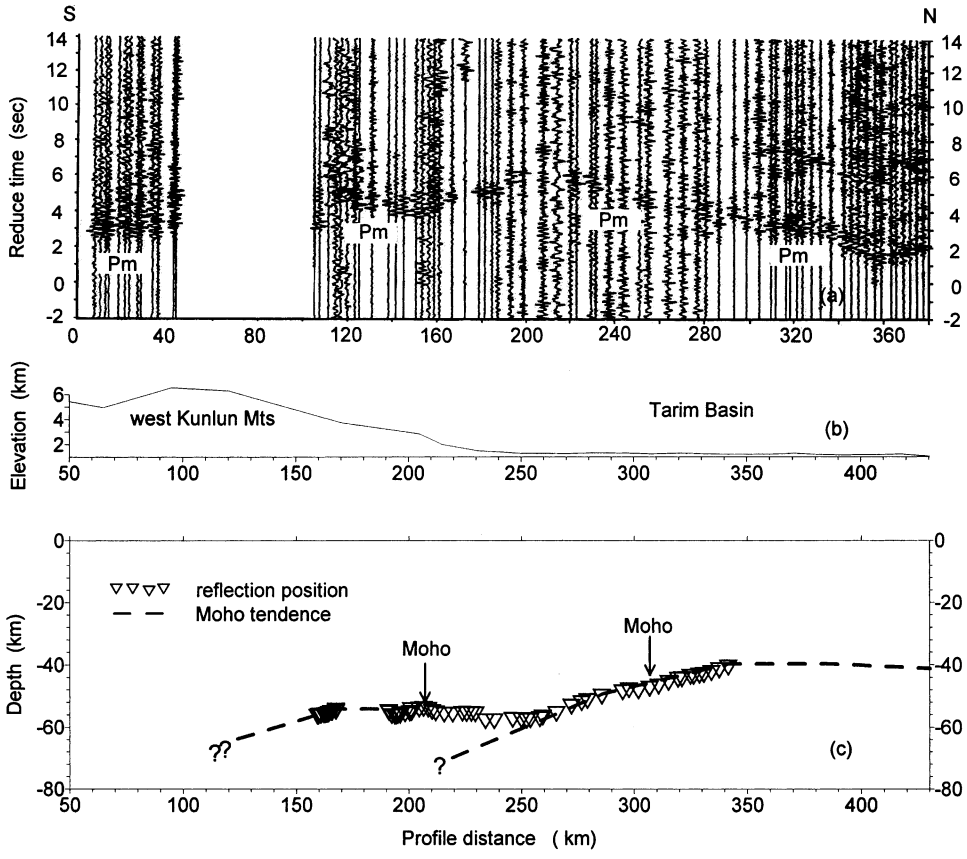


Fig. 4. Pishan shot: the record section and sketch of Moho depth (a) Fan-shaped record section derived from the Pishan shot (S10). The arrival time has been corrected to a constant offset of 160 km, on the assumption of negligible variation in the mean crustal velocity along the profile, so that it can be approximately regarded as a depth-section. Only Pm is marked in the record section. Horizontal axes: cosine of azimuth and offset; vertical axes: reduced time ($V$red. = 6.0 km s$^{-1}$). (b) Exaggerated topography along the profile. (c) A sketch of Moho variation tendency across the transition zone from Tarim to West Kunlun. Empty inverted triangles indicate the reflection position.

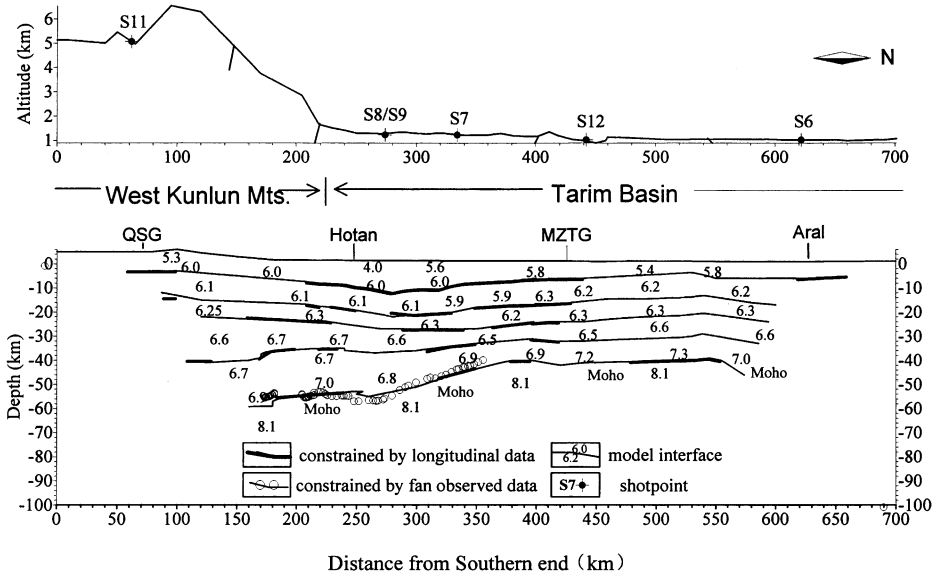


Fig. 5. A crustal structural model across the Tarim Basin to western Kunlun. The numbers are P wave velocities (in km s$^{-1}$); numbers on the vertical scale indicate depth below sea level. The upper sketch shows the topography along the profile and the projected shot-points.

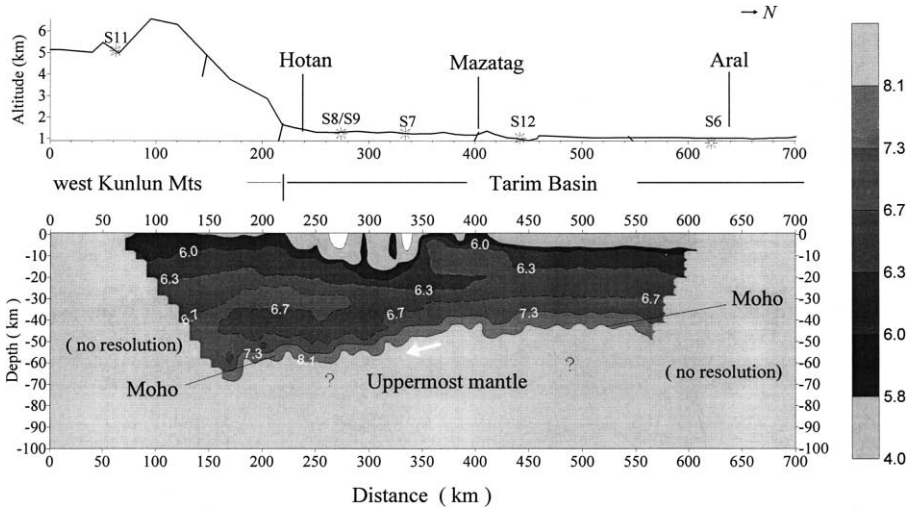


Fig. 6. The velocity contour section of the crustal model. Central Tarim: the layers are flat-lying and the velocity and thickness have no visible lateral variation. Southern Tarim: local high and low abnormality in the upper crust and subduction in the middle and lower crust. West Kunlun: obviously thick lower crust and an abnormally high-velocity middle crust.

data (Fig. 5). Due to the frequency dispersion, the resolution is higher in the upper and middle crust than in the lower crust and at Moho depth. The representative error values, of $\pm 0.1$ km s$^{-1}$ for velocity and $\pm 1$–2 km for depth, are estimated for nodes in the central part of the model, where the ray coverage was greater. As mentioned earlier, the northern portion of the model is only loosely constrained by the Aral shot data, so that there is still some uncertainty.

## 5. Crustal model: features and implications

The final velocity-depth model for the profile is shown as Fig. 5, with indications of velocity values at specific nodes, to illustrate crustal structural features beneath the transition zone between the basin and the mountains. In the model, the crystalline basement dips southward to increasing depths, from 6 to 18 km in southwest Tarim, and then rises southward, with decreasing depth, in the western Kunlun. This result coincides with that from the petroleum industry seismic profile (6 s, unpublished). The Moho depth and its lateral variation are controlled by observed data from both the longitudinal and fan-shaped records. The Moho appears to dip towards the west Kunlun Mountains at an angle between 5 and 7° with the depth below sea level increasing from 42 to 58 km. The crust has a total thickness of 42 ± 2 km in the Tarim Basin and 60 ± 2 km in the western Kunlun. Throughout the model, from north to south, the crust consists of three main layers. The upper crust, includes vertical velocity gradients and a constant layer, which is defined by velocity of $<6.3$ km s$^{-1}$ at a depth of $\sim$20 km. The middle crust consists of two layers, with a constant velocity of 62 to 6.3 km s$^{-1}$ and 6.5 to 6.7 km s$^{-1}$, from 12 to 40 km depth. The lower crust is 10–22 km thick and has a velocity ranging from 6.8 to 7.3 km s$^{-1}$.

Our model implies that there is no obvious lateral variation in the thickness of each layer within the domain of Tarim Basin, except at its southernmost margin, where the lower crust is locally thickened. On the contrary, an intense compressive deformation has occurred in area of the western Kunlun, where the basement is uplifted and thrust northward and the lower crust has been thickened to more than 20 km.

The contoured section (Fig. 6) shows the lateral and vertical variation of velocity-depth beneath our profile. The surface layer is well resolved in the segments from Hotan to Mazatag. Around the Hotan shotpoint a vertical gradient from 1.0 to 5.8 km s$^{-1}$ extends from the surface to a depth of 15 km. This indicates a huge thickness of Neozoic deposits. The high velocity recorded to the south of Hotan is associated with the Paleozoic outcrop at Tiekelik. In the central portion of the profile a local, isolated, high velocity body within the basement has been recorded on the data from the Erzhan and Sanzhan shots, whereas a low velocity layer does not appear at the depth of the middle crust beneath the Tarim Basin. This was quite unpredicted.

The mean/average velocity of 6.36 km s$^{-1}$ in the central uplift of Tarim, 6.0 km s$^{-1}$ in southwest depression of Tarim, and 6.40 km s$^{-1}$ under northern slope of the western Kunlun, is interpreted in terms of a continent–continent collision model. The high average velocity value of central Tarim implies that the crust here is relatively rigid and stable, and has not been influenced by events in Tibet. Unlike central Tarim, the high average velocity of the western Kunlun Mountains is typical of zones of crustal thickening during continent–continent collision. Low gravity values indicate incomplete isostatic compensation. The low average velocity values in southwest Tarim defines a deep and narrow foreland basin.

The hypothesis for the crustal structure beneath the

transition zone from the Tarim Basin to the western Kunlun Mountains was tested and proved by deep seismic reflection profiling, parallel to and 100 km to the east of our refraction line (CPM on Fig. 1), conducted in 1998 (Gao et al., 2000). Seismic tomography in this region (Xu et al., 2000) and seismic data constrained by gravity modeling (He et al, in preparation), support our conclusions.

## 6. Conclusions

We conclude from our results and from the discussion given above, that Tarim Basin crust has been underthrust beneath the western Kunlun. This is in agreement with the evidence in southern Tarim that both the crystalline basement and the Moho and dip southwards beneath the western Kunlun at an angle of 5–7°. The depth of the Moho increases between 10 and 15 km over a distance of 250–300 km. A further indication in support of the underthrust model is that the lower crust has been thickened to over 20 km beneath the western Kunlun, and the underlying crystalline basement has also been uplifted and thrust northwards.

An additional result of this study has been the discovery that the Central Tarim crust is stable and has great rigidity. This suggests that the core of the cratonic basin has not been affected by the collision that occurred along the northern margin of the Tibetan plate.

## Acknowledgements

Financial support was provided by Ministry of Land and Resources of the People's Republic of China (9501204), and China National 305 Project of Xinjiang Uygur Autonomous Region (96-915-07-03), China National Science Foundation (F49734230), Chinese National Key Project for Basic Research on Tibetan Plateau (G1998040800).

Borehole drilling and the firing of shots in the field was carried out by the Seismic Geological Brigade of the Seismic Bureau of Sichuan. Assistance during the writing of this paper was given by Prof. Huang Liyan and associate Profs. Li Pengwu and Guan Ye. The presentation of the paper has been improved in accordance with the suggestions of an anonymous reviewer. The English has been improved by Dr A.J. Barber.

## References

Cerveny, V., Psencik, I., 1984. SEIS83-numerical modeling of seismic wavefield in 2-D: varying layered structure by the ray method. In: Engdahl, E.R. (Ed.). Documentation of Earthquake Algorithms. Report SE-35World Data Center (A) for Solid Earth Geophysics, Boulder, CO, pp. 36–40.

Cerveny, V., Moltokov, A., Psencik, I., 1977. Ray Method in Seismology. Karlova, Prague.

Cowgill, E., Yin, A., Rumelhart, P., Foster, D., Chen, Z., Wang, X.F., 1998. Magnitude and timing of Cenozoic shortening in the W Kunlun Shan. EOS 79, F816.

Dewey, J.F., Burke, K., 1973. Tibetan, Variscan and Precambrian basement reactivation: products of continental collision. Journal of Geology 81, 683–692.

Ding, Daogui, Tang, Liangjie, 1996. Formation and Revolution of the Tarim Basin. Hehai University Press, Nanjing, pp. 11–52 (in Chinese).

Gao, Rui, Huang, Dongding, Lu, Deyuan, Qian, Guihua, Li, Yingkang, Kuang, Chaoyang, Li, Qiusheng, Li, Pengwu, Feng, Rujin, Guan, Ye, 2000. Deep seismic reflection profile across juncture zone between Tarim Basin and west Kunlun Mountain. Science Bulletin 45 (17), 1874–1879.

Jia, Chengzao (Ed.), 1997. Tectonic characteristic and Petroleum: Tarim Basin, China Petroleum Industry Press, Bejing, pp. 182–253 (in Chinese).

Layon-Caen, H., Molnar, P., 1984. Gravity anomalies and the structure of west Tibet and the southern Tarim Basin. Geophysics Research Letters 11, 1251–1254.

Liu, Xun, Fu, Derong, 1999. On the tectonic evolution of the Kunlun–Karakoram Area, Southern Xinjiang, Northwest China. Continental Dynamics 4 (2), 65–72.

Matte, Ph., Tapponnier, P., Arnaud, N., 1996. Tectonics of western Tibet between the Tarim and the Indus. Earth and Planetary Science Letters 142, 311–330.

Molnar, P., 1984. Structure and tectonics of the Himalaya: constraints and implications of geophysical data. Annual Review of Earth Planetary Science 12, 489–518.

Molnar, P., England, P., Martinod, J., 1993. Mantle dynamics, uplift of the Tibetan Plateau, and the Indian monsoon. Review of Geophysics 31, 357–396.

Nelson, K.D., et al., 1996. Partially molten middle crust beneath southern Tibet: synthesis of Project INDEPTH results. Science 274, 1684–1696.

Tapponnier, P., Peltzer, G., Armijo, R., 1986. On the mechanics of the collision between India and Asia. Collision Tectonics, Coward, M.P., Ries, A.C. (Eds.). Geological Society of London Special Publication vol. 19, 115–157.

Xu, Yi, Liu, Futian, Liu, Jianhua, et al., 2000. The seismic tomography of the continental orogenic belt and its abutting basin in northwestern China. Science in China 30 (2), 113–122.

Yuan, X., Ni, J., Kind, R., Mechie, J., Sandvol, E., 1997. Lithospheric and upper mantle structure of southern Tibet from a seismological passive source experiment. Journal of Geophysical Research 102, 27491–27500.

Zhao, W.J., Nelson, K.D., INDEPTH team, 1993. Deep seismic evidence for continental underthrusting beneath Tibet. Nature 366, 557–559.